

Domain-wall transformation by high-frequency magnetic fields

Andreas Neudert,* Jeffrey McCord, Rudolf Schäfer, and Ludwig Schultz

Leibniz Institute for Solid State and Materials Research, IFW Dresden, Helmholtzstrasse 20, D-01069 Dresden, Germany

(Received 19 March 2007; published 18 May 2007)

The high-frequency behavior of magnetic domain-walls of the cross-tie type is investigated by static and time-resolved Kerr microscopy. By applying a high-frequency (hf) sinusoidal in-plane magnetic field perpendicular to the wall plane, additional vortex-antivortex pairs are created that lead to a shrinking of the cross-tie spacing. This creation of additional Bloch lines happens by a channelized flux transport across the wall plane at the vortex sites until a new metastable narrow-spaced cross-tie state is reached.

DOI: [10.1103/PhysRevB.75.172404](https://doi.org/10.1103/PhysRevB.75.172404)

PACS number(s): 75.40.Gb, 75.60.Ch

The internal domain-wall structure in magnetic films depends on anisotropy and film thickness. For thin films (thinner than about 30 nm in case of $\text{Ni}_{81}\text{Fe}_{19}$), 180° domain walls are of the symmetric Néel wall type, where the rotation of magnetization occurs in the plane of the film.¹ As there is a nonvanishing divergence of magnetization, dipolar magnetic charges are found across the domain wall. This leads to an increase of the specific wall energy with increasing thickness. For thick films (thicker than approximately 100 nm in the case of $\text{Ni}_{81}\text{Fe}_{19}$), asymmetric Bloch walls are energetically favored.² There, the change of magnetization is realized by an in-plane vortex structure along the wall axis, leading to an almost stray-field-free magnetization distribution. In an intermediate thickness range, a third domain-wall type is found that consists of a network of orthogonal 90° Néel walls with alternating wall magnetization direction (Fig. 1). This structure is called cross-tie wall.³ The individual Néel wall segments are connected by vortices and antivortices (also called circular and cross Bloch lines, respectively). The additional transverse Néel walls emerging from the antivortices reach several micrometers into the two domains next to the cross-tie wall.

The cross-tie spacing λ depends on the strength of the magnetic anisotropy (parallel to the wall axis), the interaction of the 90° Néel wall segments, and on the self-energy of the Bloch lines.⁵ λ decreases either with increasing magnitude of the longitudinal anisotropy or with increasing thickness. The reason for the latter is the decreasing self-energy of the Bloch lines with increasing thickness.⁶ The wall shown in Fig. 1 with a cross-tie spacing of about $15 \mu\text{m}$ represents the magnetic ground state that was obtained by degaussing the sample in an external ac magnetic field of decreasing amplitude at a moderate frequency, oriented transverse to the wall direction.

In Ref. 7, we reported on the multiplication of Bloch lines in cross-tie walls due to the influence of a repetitive pulsed magnetic field applied transversely to the wall direction. In that paper, we applied this pulsed field using different repetition rates. These experiments indicated that the cross-tie spacing depends on the frequency of the excitation. This frequency dependence is investigated in this Brief Report using *sinusoidal* field excitation that allows us to excite the cross-tie wall with a single frequency and not with a broad spectrum of different frequencies, as in the case of the pulsed field excitation. Using this single frequency excitation, we found additional insights in the mechanism of cross-tie mul-

tiplication in walls excited by high-frequency (hf) magnetic fields.

To excite the magnetic microstructure using in-plane hf magnetic fields, the elements are deposited on top of a coplanar waveguide structure. A hf sinusoidal voltage applied to this waveguide structure results in a hf magnetic field around the center conductor. We used two different illumination sources. Either a continuous wave (cw) emitting Xe arc lamp or a pulsed laser that was in phase with the excitation field. Using the cw illumination, which is by definition not time resolving, allowed us to excite the sample with frequencies that are not a multiple of the laser repetition rate of 23 MHz. Although these images show an averaged state of the magnetization in the sample, the cross-tie spacing could still be extracted from the images due to the low mobility of the antivortex. Time-resolved images can be acquired using the pulsed laser illumination method with in-phase excitation of the magnetic sample. Thus, a temporal resolution of about 50 ps can be achieved. The sizes of the elements are 160×80 and $80 \times 40 \mu\text{m}^2$, respectively. The thickness of the $\text{Ni}_{81}\text{Fe}_{19}$ film is 50 nm to support the formation of a cross-tie wall in the demagnetized state (see Fig. 1). Details of the film deposition and element structuring process are described elsewhere.⁸

By applying a sinusoidal field (peak-to-peak amplitude 200 A/m) to the magnetic ground state shown in Fig. 1, the average cross-tie distance or wavelength decreases. To avoid any influence of disturbing voltage spikes during changing the frequency of the sine generator or by enabling and/or disabling the output channel, each investigated domain state was produced as follows. The hf magnetic field was applied to the sample and then the sample was demagnetized in a damped, slowly oscillating field of about 80 Hz applied par-

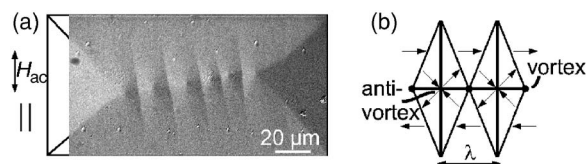


FIG. 1. (a) Kerr micrograph of the demagnetized state in a $160 \times 80 \mu\text{m}^2$ sized $\text{Ni}_{81}\text{Fe}_{19}$ rectangle (thickness 50 nm) with a cross-tie wall in the center of the element. A domain scheme (Ref. 4) of the magnetization orientation in a cross-tie wall is shown in (b).

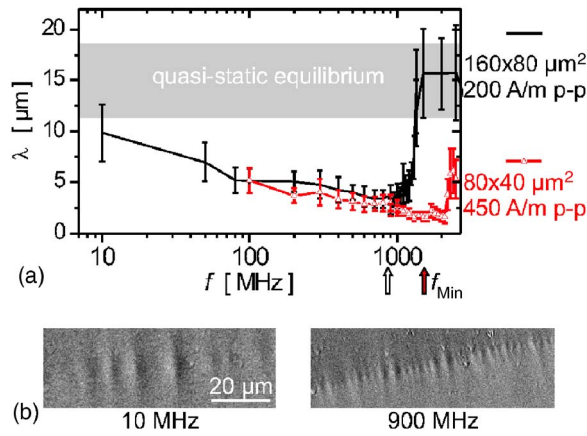


FIG. 2. (Color online) (a) Change of cross-tie wavelength with respect to the frequency of the sinusoidal in-plane field excitation in a $160 \times 80 \mu\text{m}^2$ (peak-to-peak amplitude 200 A/m) and $80 \times 40 \mu\text{m}^2$ (450 A/m) sized rectangular element of 50 nm thickness. The quasistatic cross-tie spacing shown in Fig. 1 is shaded for comparison ($\lambda_{\text{av}} \pm \lambda_{\text{sd}}$; average: $\lambda_{\text{av}} = 15.1 \mu\text{m}$, standard deviation: $\lambda_{\text{sd}} = 3.6 \mu\text{m}$). Exemplary images of the wall in the bigger element at 10 and 900 MHz are shown in (b). The partially blurred wall contrast at 10 MHz indicates a strong vortex motion in the outer parts of the cross-tie wall.

allel to the short edge of the rectangular element. The initial amplitude of this oscillating field was larger than the saturation field. After reducing the amplitude of the 80 Hz field, the image of the actual domain state was acquired using the above-mentioned cw illumination for static wide-field Kerr microscopy (due to the small hf excitation, the oscillating magnetic structures appear fuzzy in the images). Then this process was repeated for the next frequency. This procedure ensures that the magnetic state of the element is in a dynamic equilibrium, as given by the influence of the applied hf field.

Using this method, a minimal cross-tie spacing of about $4 \mu\text{m}$ at 900 MHz in the $160 \times 80 \mu\text{m}^2$ sized element was reached. The cross-tie wavelength with respect to the excitation frequency is shown in Fig. 2(a). With increasing frequency, the cross-tie spacing decreases to a minimum at f_{min} and at frequencies larger than f_{min} , a sharp increase toward the quasistatic spacing is found. For the smaller, $80 \times 40 \mu\text{m}^2$ sized element of same thickness we found a smaller minimal λ at a higher frequency $f_{\text{min}} = 1600 \text{ MHz}$, compared to $f_{\text{min}} = 900 \text{ MHz}$ for the $160 \times 80 \mu\text{m}^2$ sized element. As the resonance frequency of the magnetization depends on the local effective field, the smaller element reveals a higher resonance frequency for the magnetization in the domains due to a stronger demagnetizing field.⁹ This leads to the higher frequency f_{min} . Increasing the amplitude at a fixed frequency resulted in a smaller cross-tie spacing, if the frequency was lower than f_{min} , but it did not change the frequency position of the smallest cross-tie spacing f_{min} .

The dynamic processes in the $160 \times 80 \mu\text{m}^2$ sized element have further been investigated using time-resolved wide-field Kerr microscopy. For details of the time-resolved experiment, we refer to Ref. 8. The pulsed field excitation described in that paper⁸ was replaced by a sinusoidal excitation, which was phase locked to the laser pulses. This was

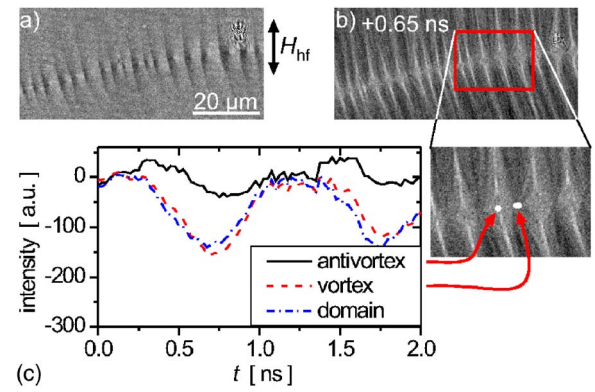


FIG. 3. (Color online) Excitation of the cross-tie wall in the $160 \times 80 \mu\text{m}^2$ sized element using a 922 MHz, 180 A/m peak-to-peak hf magnetic field. In (a), the domain image of the cross-tie wall at $t = 0 \text{ ns}$ is shown ($\lambda_{\text{av}} = 4.0 \mu\text{m}$, $\lambda_{\text{sd}} = 1.1 \mu\text{m}$). The difference image in (b) is taken at the time of maximum elongation of magnetization (0.65 ns) in the domains next to the cross-tie wall. The averaged Kerr intensity of the difference images ($\sim \Delta m$) at the sites of vortex, antivortex, and within the domain, respectively, is plotted in (c) at the positions indicated by arrows. The change of magnetization (i.e., the transport of magnetic flux across the wall) is by a factor of 2 larger at the vortex position than at the antivortex position.

achieved by using a voltage-controlled oscillator that was stabilized by a phase-locked loop (PLL). Due to the fixed amplitude of the oscillator, the resulting amplitude after amplification (using a fixed amplifier and a set of fixed attenuators) was 180 A/m instead of the 200 A/m used for the experiment shown in Fig. 2. The frequency was set to 922 MHz, which is in the region of the smallest cross-tie spacing shown in Fig. 2. The change of magnetization Δm in the vicinity of the cross-tie wall due to this sinusoidal excitation is shown by a difference image in Fig. 3(b) with the state of Fig. 3(a) as a background image. The time dependence of Δm is analyzed at the position of a vortex, of an antivortex, and within the domains, respectively, and plotted in Fig. 3(c). The change of magnetization around the antivortex is about a factor of 2 smaller than compared to the magnetization around the vortex. Also, a phase shift between the vortex and antivortex sites can be noted. The response at the antivortex position is lagging behind, compared to the response of the magnetization at the vortex position. This phase shift is due to the lower mobility of the antivortex compared to the vortex. The response of the vortex is in phase with the excitation of the magnetization in the domains as well as the amplitude of the response of the magnetization.

The main questions arising from this experimental observations are as follows: Why is the cross-tie spacing decreasing with increasing frequency and how are the additional vortex-antivortex pairs created?

To offer an explanation for the dynamic processes, it is helpful to describe the response of a cross-tie wall to a quasistatic applied magnetic field, as shown in Fig. 4. By applying the magnetic field perpendicular to the wall plane (as indicated), the vortices move to the right, whereas the antivortices stay at their positions. The local susceptibility of the

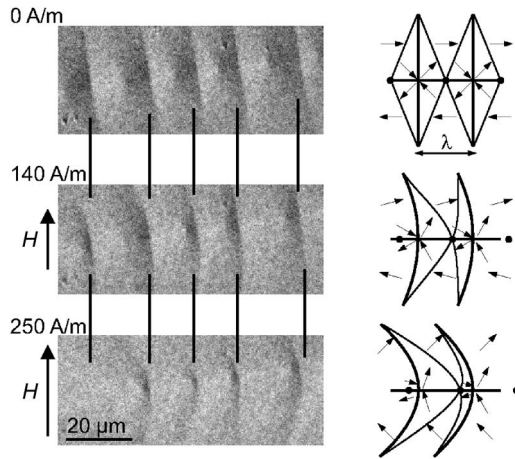


FIG. 4. Reaction of the cross-tie wall in the $160 \times 80 \mu\text{m}^2$ sized element to a quasistatically applied magnetic field. The magnetization distribution is sketched next to the images.

wall is larger at a vortex site than at the position of an antivortex. This is due to the charges of the transverse Néel walls that emerge from the antivortices. These magnetic charges stiffen the magnetization in the vicinity of the antivortex, which leads to a greater mobility of the vortices compared to the antivortices. Due to the additional rotation of the magnetization located between the transverse Néel walls, these walls are bending to prevent the generation of additional magnetic charges. The motion of the vortices increases the length of the Néel wall sections that possess a magnetization component parallel to the applied field. This enables the magnetic flux, that is created by the rotation of magnetization in the domains next to the wall, to be transported across the wall. Thus, the flux transport is realized by a motion of the vortices perpendicular to the applied field axis, as shown in Fig. 5, for a quasistatic field of small amplitude.

The dynamic processes are related to this quasistatic description. Assume the initial, wide-spaced cross-tie state as starting configuration. In the presence of the hf field, the magnetization in the domains next to the cross-tie wall is oscillating with the same frequency. This means that a transverse component of magnetic flux is created next to the wall that has to be transported across the wall plane to avoid magnetic charges. Like in the quasistatic case, the vortices possess a higher mobility than the antivortices, which can also be seen in the plot (c) in Fig. 3 for the hf field excitation, where the time-dependent Kerr intensity is plotted for the vortex and antivortex locations.

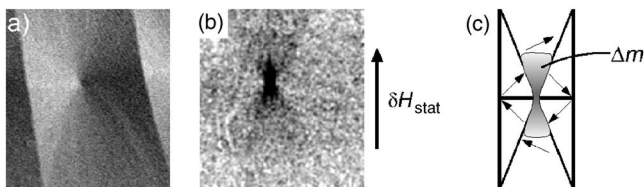


FIG. 5. Transport of magnetic flux across a cross-tie wall. The change of magnetization of a wide-spaced cross-tie state (a) by a small perturbation δH is shown in the difference image (b). The localized area of flux transport is sketched in (c).

The magnetization rotation in the 180° domains takes place at the frequency of the hf excitation field, as it is not a free oscillation but a forced one. Consequently, also the flux transport across the wall has to take place at the same frequency. Therefore, the vortex will be driven by a frequency that is larger than the eigenfrequency of the lateral mode of a vortex in this sample, which is in the sub-100 MHz range, as shown in Fig. 2(b) and in Refs. 10 and 11. For smaller elements, the frequencies of the transversal motion of the vortex are in the 100 MHz region.^{12–14} The amplitude of the vortex oscillation is strongly reduced, as it is excited with frequencies larger than its eigenfrequency. Therefore, it is favorable to create additional vortex-antivortex pairs, as the transport of magnetic flux happens mainly at the vortex sites. By increasing the number of vortices in the wall, the amount of flux that can be transported across the wall plane increases, although each individual vortex oscillates at relative low amplitude. This increased vortex-antivortex density leads to a smaller cross-tie spacing and, thus, the transverse Néel walls are closer together, which increases the local charge density along the wall. Due to the increased charge density, the internal fields between these transverse walls increase which will stiffen the wall magnetization and result in a decreased amplitude of the magnetization oscillation. The decreased amplitude of the oscillation reduces also the probability of a vortex-antivortex nucleation and a metastable state is reached. By increasing the amplitude or frequency of the excitation field, the amplitude of the magnetization oscillation in the domains increases and, consecutively, also the probability of the creation of an additional vortex-antivortex pair. This model explains qualitatively the decrease of λ with increasing frequency (shown in Fig. 2) or increasing amplitude (not shown).

As recently shown by Waeyenberge *et al.*,¹⁵ the magnetic microstructure of a vortex undergoing an excitation by fast magnetic fields is disturbed so that it cannot be described by the rigid vortex model.¹⁶ They also showed the nucleation of a second vortex and an antivortex. The antivortex and the initial vortex annihilated each other so that the final magnetic state consisted again of a single vortex in the element. In contrast to the observations reported in Ref. 15, in the rectangular-shaped elements investigated here, the vortex-antivortex pair is (meta)stable. This leads to an increased number of vortex-antivortex pairs in the domain wall and thus to a reduced cross-tie spacing. The high-density metastable state of the cross-tie wall can only be resolved by demagnetizing the sample in an external field which is large enough to destroy the wall.

The increased stability of the additional vortex-antivortex pairs found in our sample can be explained by the larger size and different shape of our elements, which reduces the strength of the effective internal field, whereas in the case of the smaller quadratic elements in Ref. 15 ($1.5 \mu\text{m}$ vs $80 \mu\text{m}$) the stronger demagnetizing field prohibits the existence of a vortex-antivortex pair additional to the already existing vortex. In fact, this would be a short section of a cross-tie wall, which is not stable in such small elements.

For frequencies higher than f_{min} , the resonance frequency of the magnetization in the domains is exceeded and, therefore, the amplitude of the magnetic oscillation and the

amount of magnetic flux that are transported across the wall plane are reduced. Consecutively, the probability of a vortex-antivortex pair generation is also reduced and the cross-tie spacing increases with increasing frequency. For even higher frequencies, the dynamic susceptibility of the magnetization shrinks to zero and the wall structure is unchanged.

To answer the two questions posed above, the additional vortex-antivortex pairs are created by a driven oscillation of an existing vortex in the vicinity of the local internal fields caused by the interaction of the main Néel wall segments

with the transverse Néel walls. And the energetic reason for this creation is the increased flux transport across the wall plane via the vortex sites. Otherwise, magnetic charges would be created in the sample and this would lead to an increase of stray-field energy.

We thank R. Kunze for lending of the hf sine generator and amplifier and B. Lange for the PLL stabilized oscillator. Financial support by the DFG priority program SPP 1133 “Ultrafast magnetization processes” is gratefully acknowledged.

*Present address: School of Physics, University of Exeter, Stocker Road, Exeter, Devon EX4 4QL, UK. Electronic address: a.neudert@exeter.ac.uk

¹L. Néel, Acad. Sci., Paris, C. R. **241**, 533 (1955).

²A. Hubert, Phys. Status Solidi **32**, 519 (1969).

³E. E. Huber, Jr., D. O. Smith, and J. B. Goodenough, J. Appl. Phys. **29**, 294 (1958).

⁴A. Holz and A. Hubert, Z. Angew. Phys. **26**, 145 (1969).

⁵S. Middlehoek, J. Appl. Phys. **34**, 1054 (1963).

⁶H. Bäurich, Phys. Status Solidi **23**, K137 (1967).

⁷A. Neudert, J. McCord, R. Schäfer, R. Kaltoven, I. Mönch, H. Vinzelberg, and L. Schultz, J. Appl. Phys. **99**, 08F302 (2006).

⁸A. Neudert, J. McCord, D. Chumakov, R. Schäfer, and L. Schultz, Phys. Rev. B **71**, 134405 (2005).

⁹C. Kittel, Phys. Rev. **73**, 155 (1948).

¹⁰K. Y. Guslienko, B. A. Ivanov, V. Novosad, Y. Otani, H. Shima,

and K. Fukamichi, J. Appl. Phys. **91**, 8037 (2002).

¹¹A. Neudert, J. McCord, R. Schäfer, and L. Schultz, J. Appl. Phys. **97**, 10E701 (2005).

¹²K. S. Buchanan, P. E. Roy, M. Grimsditch, F. Y. Fradin, K. Y. Guslienko, S. D. Bader, and V. Novosad, Nat. Phys. **1**, 172 (2005).

¹³J. P. Park, P. Eames, D. M. Engebretson, J. Berezovsky, and P. A. Crowell, Phys. Rev. B **67**, 020403(R) (2003).

¹⁴V. Novosad, F. Y. Fradin, P. E. Roy, K. S. Buchanan, K. Y. Guslienko, and S. D. Bader, Phys. Rev. B **72**, 024455 (2005).

¹⁵B. van Waeyenberge, A. Puzic, H. Stoll, K. W. Chou, T. Tylliszczak, R. Hertel, M. Fähnle, H. Brückl, K. Rott, G. Reiss, I. Neudecker, D. Weiss, C. H. Back, and G. Schütz, Nature (London) **444**, 461 (2006).

¹⁶K. Y. Guslienko, V. Novosad, Y. Otani, H. Shima, and K. Fukamichi, Appl. Phys. Lett. **78**, 3848 (2001).